Title

Dynamic Microtubules Drive Circuit Rewiring in the Absence of Neurite Remodeling

Journal

Current Biology, 25(12)

ISSN

0960-9822

Authors

Kurup, Naina

Yan, Dong

Goncharov, Alexandr

et al.

Publication Date

2015-06-01

DOI

10.1016/j.cub.2015.04.061

Peer reviewed

HHS Public Access

Author manuscript

Curr Biol. Author manuscript; available in PMC 2016 June 15.

Published in final edited form as:

Curr Biol. 2015 June 15; 25(12): 1594–1605. doi:10.1016/j.cub.2015.04.061.

Dynamic microtubules drive circuit rewiring in the absence of neurite remodeling

Naina Kurup[1], **Dong Yan**[1,4], **Alexandr Goncharov**[2], and **Yishi Jin**[1,2,3,*]

[1]Neurobiology Section, Division of Biological Sciences, University of California, San Diego, La Jolla CA 92093, USA

[2]Howard Hughes Medical Institute, University of California, San Diego, La Jolla CA 92093, USA

[3]Department of Cellular and Molecular Medicine, University of California, San Diego, La Jolla CA 92093, USA

Abstract

A striking neuronal connectivity change in *C. elegans* involves the coordinated elimination of existing synapses and formation of synapses at new locations, without altering neuronal morphology. Here, we investigate the tripartite interaction between dynamic microtubules (MTs), kinesin-1, and vesicular cargo during this synapse remodeling. We find that a reduction in the dynamic MT population in motor neuron axons, resulting from genetic interaction between loss of function in the conserved MAPKKK *dlk-1* and an α-tubulin mutation, specifically blocks synapse remodeling. Using live imaging and pharmacological modulation of the MT cytoskeleton, we show that dynamic MTs are increased at the onset of remodeling and are critical for new synapse formation. DLK-1 acts during synapse remodeling, and its function involves MT catastrophe factors including kinesin-13/KLP-7 and spastin/SPAS-1. Through a forward genetic screen, we identify gain-of-function mutations in kinesin-1 that can compensate for reduced dynamic MTs to promote synaptic vesicle transport during remodeling. Our data provide *in vivo* evidence supporting the requirement of dynamic MTs for kinesin-1 dependent axonal transport and shed insight on the role of the MT cytoskeleton in facilitating neural circuit plasticity.

Graphical Abstract

*Corresponding author: yijin@ucsd.edu, 858-534-7754 (phone), 858-534-7773 (fax).

[4]Present address: Department of Molecular Genetics and Microbiology, Duke University School of Medicine, Durham, NC 27710, USA

Author Contributions

N. K. designed, interpreted and performed experiments and wrote the paper, D. Y. designed and performed the *tba-1(gf) dlk-1(0)* suppressor screen, A. G. performed EM analyses and Y. J. designed and interpreted experiments and wrote the paper.

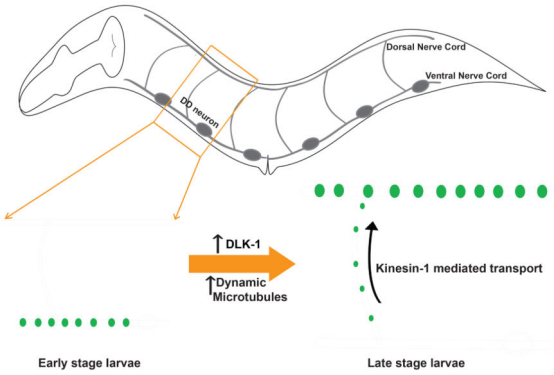

Keywords

MT dynamics; DLK-1; kinesin-1; synaptic vesicle transport

Introduction

Neural circuits undergo connectivity changes in response to various stimuli throughout the lifetime of an organism. Such changes can occur at many levels, including neurite growth and pruning, synapse formation and elimination, as well as strengthening and weakening of existing synapses [1]. Such structural plasticity is highly dependent on the cytoskeletal architecture of the neuron. Microtubules (MTs) are essential for neuronal polarity, neurite outgrowth and guidance [2]. Studies of the *Drosophila* neuromuscular junction (NMJ), where MTs form loops within terminal synaptic boutons, have shown that Microtubule Associated Proteins (MAPs) like Futsch [3, 4] and Spartin [5] regulate synapse growth by modulating MT stability. In the mammalian central nervous system, many synapses are formed *en passant* along the axons of neighboring nerve processes [6]. In such neurons, where MTs generally run parallel to synapse boutons within the axon, how MTs affect synapse formation and maintenance remains to be understood.

In this study, we investigated how MTs affect the developmental rewiring of *C. elegans* GABAergic DD (Dorsal D type) neurons, referred to as DD remodeling [7]. Six DD motor neurons are positioned along the ventral nerve cord and extend neurites in ventral and dorsal nerve cords, connected by circumferential commissures [8]. In the first larval (L1) stage, DD neurons form *en passant* synapses with the ventral body wall muscles. By the end of the second larval (L2) stage, these ventral synapses are eliminated, and new synapses are formed onto the dorsal body wall muscles, which are maintained for the rest of the lifetime of the animal [8-11]. Importantly, the remodeling of synapses does not involve changes in axon morphology [10]. Thus, the elimination and reformation of synapses would possibly require the coordinated action of vesicular sorting and transport pathways, together with modifications in the underlying cytoskeleton. Recent work has shown a cyclin dependent kinase functions to promote new synapse formation in the dorsal neurites of the DD neurons, via the regulation of motor proteins UNC-104 (Kinesin-3) and DHC-1(Dynein) [11]. However, whether cytoskeletal changes are necessary for DD remodeling remains unknown.

The conserved DLK (Dual-Leucine zipper bearing MAP3K) family of kinases (DLK-1 in *C. elegans*) regulates several aspects of neuronal development and maintenance, including synapse and axon development, neuronal survival and axon regeneration [12-18]. In *C. elegans*, DLK-1 regulates synapse development, neurite outgrowth and regeneration via a p38 MAP kinase pathway, with the transcription factor CEBP-1 as a downstream target [12, 13]. Additionally, MT associated proteins (MAPs) such as the kinesin-13 homolog *klp-7* [15], have also been implicated in DLK-1 signaling in developing and mature neurons.

Recent studies in a variety of neuronal models have identified context-specific roles of DLK homologs in regulating MTs [16-18]. Here, using a gain-of-function mutation in α-tubulin (designated *tba-1(gf)*) [19] to perturb the MT cytoskeleton in animals lacking DLK-1 activity (designated *dlk-1(0)*), we have uncovered a specific role for DLK-1 and dynamic MTs in synapse remodeling. Remodeling is blocked in *tba-1(gf) dlk-1(0)* double mutants and transient expression of *dlk-1* during DD remodeling is sufficient to establish new synapses. Upregulation of MT dynamics is correlated with the onset of synapse remodeling, and increasing the number of dynamic MTs can rescue the block in remodeling in *tba-1(gf) dlk-1(0)*. We further identified novel kinesin-1 mutations that facilitate synaptic vesicle transport during remodeling in *tba-1(gf) dlk-1(0)*, likely through an increase in the MT binding affinity of the motor. Our findings demonstrate that dynamic MTs promote neural circuit remodeling, independent of neurite outgrowth.

Results

DD remodeling depends on the MT cytoskeleton and DLK-1

tba-1(ju89) (*tba-1(gf)*) is a gain-of-function mutation that converts a glycine residue to arginine (G414R) in the C-terminal H11-H12 loop of the α-tubulin TBA-1, causing a mild disruption of synapse morphology and a reduction in synapse number [19]. To test whether *tba-1(gf)* also affected DD remodeling, we examined the localization pattern of a DD neuron-specific synaptic marker (*juIs137*: $P_{flp\text{-}13}$-SNB-1::GFP). In wild type animals grown at 20°C, DD remodeling was completed by the end of the second larval (L2) stage (~28 hrs post hatching, hph), but in *tba-1(gf)* animals remodeling was not completed until adulthood (~56 hph) (Figure S1A), suggesting that an altered MT cytoskeleton delayed synapse remodeling.

To understand how MTs regulate synapse remodeling, we searched for genetic interactors of *tba-1(gf)*. We found that loss of the MAPKKK DLK-1 (*dlk-1(0)*), together with *tba-1(gf)*, resulted in a striking synergistic effect on DD remodeling. In L1 animals of wild type, *tba-1(gf)*, *dlk-1(0)* single and *tba-1(gf) dlk-1(0)* double mutants, DD neurons formed synapses along the ventral nerve cord (VNC) (Figure 1A, C). By the adult stage, DD neurons in wild type, *tba-1(gf)* and *dlk-1(0)* single mutants remodeled their synapses and formed new synapses along the dorsal nerve cord (DNC) (Figure 1B, C). In contrast, *tba-1(gf) dlk-1(0)* adults showed a complete lack of synaptic puncta in the DNC, and retained synaptic puncta in the VNC (Figure 1B, C). In >80% of adult *tba-1(gf) dlk-1(0)* animals, synaptic puncta were also retained in the commissures of DD neurons (n> 50 animals) (Figure 1B), suggestive of a failure in synaptic vesicle transport. *tba-1(gf)* animals exhibit mild axon outgrowth defects [19], which were not enhanced by *dlk-1(0)* (Figure

S1C, D), indicating that the synapse remodeling defect of *tba-1(gf) dlk-1(0)* was not caused by defects in axon outgrowth. The failure in DD remodeling in *tba-1(gf) dlk-1(0)* was also observed using markers for other presynaptic components, including SAD-1 and RAB-3 (Figure S1G). However, the gross clustering pattern of postsynaptic $GABA_A$ receptors (UNC-49) in the dorsal muscles was normal in *tba-1(gf) dlk-1(0)* (Figure S1G), indicating that the failure in synapse remodeling was restricted to pre-synaptic terminals.

To further characterize the anatomical changes in DD neuron pre-synaptic terminals, we performed ultrastructural analyses of DD neuron processes in young L1 and adult animals, identified by their stereotypic position within the nerve cords [8]. We observed comparable numbers of *en passant* DD neuron synapses (defined as synaptic vesicles clustered around an electron dense region called active zone) in the VNC of L1 wild type and *tba-1(gf) dlk-1(0)* animals (~6 synaptic boutons/10 μm; n=2 animals per genotype). In contrast, while the DNC of two WT adults contained 5 and 7 DD synaptic boutons in the 8 μm serially reconstructed, we observed only one dorsal DD synaptic bouton each in both *tba-1(gf) dlk-1(0)* animals reconstructed, which also contained significantly fewer vesicles than wild type (Figure 1D, E). Neither WT nor *tba-1(gf) dlk-1(0)* animals contained any recognizable DD synaptic boutons in the VNC. These studies provide further evidence that DD remodeling is severely impaired in *tba-1(gf) dlk-1(0)* animals.

The block in DD remodeling caused a distinct behavioral deficit in adult *tba-1(gf) dlk-1(0)* animals. *tba-1(gf)* animals exhibit altered locomotion with reduced velocity and sinusoidal amplitude [19], compared to wild type or *dlk-1(0)* animals (Figure 1F, Figure S1B). *tba-1(gf) dlk-1(0)* double mutant animals displayed a curved body shape during forward locomotion (Figure 1F) and coiled dorsally when prompted to move backwards (Movie S1). This synergistic interaction was specific to *dlk-1(0)* and *tba-1(gf)*, as *tba-1(0)* and *tba-1(0) dlk-1(0)* animals showed no detectable defects in locomotion and DD synapse organization (Figure S1E, F). Moreover, expression of wild type *dlk-1* or *tba-1* in the D motor neurons rescued the dorsal coiling and synapse remodeling defects in *tba-1(gf) dlk-1(0)* (Figure 1G, H), consistent with previous conclusions that DLK-1 and TBA-1 act cell-autonomously [12, 19]. Together, these data identify a previously unknown role for *dlk-1* and the MT cytoskeleton in promoting DD remodeling.

DLK-1 promotes new synapse formation during DD remodeling

We next addressed how the timing of DD remodeling was affected by *tba-1(gf)* and *dlk-1(0)* through developmental time-course studies. In wild type animals (grown at 20°C), synapses of DD neurons initially formed with ventral body wall muscles, were eliminated starting in late L1, and new synapses were formed with dorsal body wall muscles by late L2 [9-11] (Figure 2A). *dlk-1(0)* animals displayed a short delay in forming new synapses in the dorsal neurites of DD neurons, resembling the delay seen in *tba-1(gf)* animals (Figure 2A, S1A). In *tba-1(gf) dlk-1(0)* animals, a few dorsal synaptic puncta of reduced intensity were present from the L2-L4 stage, but adult animals lacked detectable synapses in the dorsal DD processes (Figure 2A, B).

To test the temporal requirement for *dlk-1* activity during DD remodeling, we induced its expression at different developmental stages using a heat shock promoter driven *dlk-1*

construct. Inducing *dlk-1* expression in larval or adult wild type animals did not cause remodeling defects (Figure 2C). When *dlk-1* was induced in *tba-1(gf) dlk-1(0)* during DD remodeling (22 hph), >70% of the animals eliminated synapses to the ventral body muscles and formed new synapses with dorsal body wall muscles, which were maintained to adulthood (Figure 2C, D). Moreover, *dlk-1* induction in any other developmental stage did not result in the retention of transient synapses observed in the dorsal DD neuron processes of L2-L4 *tba-1(gf) dlk-1(0)* animals (Figure 2A, B), indicating that *dlk-1* activity was primarily required for formation, not maintenance, of new synapses (Figure 2C, D). Thus, transient expression of *dlk-1* in the L2 stage is required for establishing new synapses during DD remodeling.

DLK-1 regulates DD remodeling through p38/PMK-3 and MT catastrophe factors

Previous studies have established that DLK-1 signals via the p38 MAP kinase PMK-3, the MAPK activated kinase MAK-2 and the transcription factor CEBP-1 to co-ordinate synapse formation [12, 13]. To test if DLK-1 acts through the same downstream genes to promote DD remodeling, we constructed double mutants of *tba-1(gf)* with *pmk-3(0)*, *mak-2(0)* and *cebp-1(0). tba-1(gf); pmk-3(0)* completely blocked DD remodeling, and retained synaptic puncta in the VNC, indistinguishable from *tba-1(gf) dlk-1(0)* animals (Figure 3A, D). *tba-1(gf); pmk-3(0)* animals also coiled dorsally during backward movement like *tba-1(gf) dlk-1(0)* animals (data not shown). However, in *tba-1(gf); mak-2(0)* and *tba-1(gf); cebp-1(0)* adult animals, we observed DD synaptic puncta in the DNC, and the number of synapses in the double mutant animals was similar to that of *tba-1(gf)* single mutants (Figure S2A). Thus DD remodeling proceeded normally in *cebp-1* or *mak-2* mutant animals, suggesting that DLK-1 functions through other downstream genes.

The MT depolymerizing kinesin-13 (KLP-7) was previously found to act downstream of the DLK-1 pathway in axon regeneration [15]. To test whether KLP-7 acted in synapse remodeling, we examined its interaction with *tba-1(gf). tba-1(gf); klp-7(0)* double mutants displayed impaired DD remodeling, partially resembling *tba-1(gf) dlk-1(0)* (Figure 3B, D). The partial remodeling defects of the *tba-1(gf); klp-7(0)* animals also suggested that the DLK cascade might act via multiple MAPs in regulating synapse remodeling. We further tested several other MAPs and found that loss of the MT severing protein spastin (SPAS-1) [20] also synergized with *tba-1(gf)* to impair DD remodeling (Figure 3C, D), whereas loss of MT stabilizing proteins like doublecortin (ZYG-8) [21] and EMAP (ELP-1) [22] did not (data not shown). Taken together, these results suggest that DLK-1 acts through PMK-3 and MT catastrophe factors like KLP-7 and SPAS-1 to regulate DD remodeling.

Dynamic MTs are reduced in *tba-1(gf) dlk-1(0)*

To understand how the interaction between *tba-1(gf)* and *dlk-1(0)* affected the MT cytoskeleton, we first assessed gross changes in MT composition. Analyses of whole-mount immunostaining using antibodies against total tubulin and a variety of microtubule post-translational modifications (MT-PTMs) [23] showed no significant changes in the nerve cords of *tba-1(gf) dlk-1(0)* (Figure S3A-E), although subtle changes in DD neurons could be masked by the presence of other neurites [8].

To directly visualize MTs in DD neurons, we next examined the ultrastructure of the MT cytoskeleton preserved using high pressure freeze fixation. We collected transverse sections of both nerve cords. In wild type and *dlk-1(0)* animals, MTs predominantly ran longitudinally along the axon, their cross-section appearing as concentric circles in transverse sections (Figure S4A). In *tba-1(gf)* animals we observed an additional population of misoriented MTs, oriented parallel to transverse sections (Figure S4A, S4B). In *tba-1(gf) dlk-1(0)* there was an overall increase in the number of axonal MTs (Figure 4B), but significantly fewer misoriented MTs than in *tba-1(gf)* alone (Figure S4B). There was also a two-fold increase in the number of synaptic MTs in *tba-1(gf), dlk-1(0)* and *tba-1(gf) dlk-1(0)* when compared to wild type (Figure 4B). We further analyzed MT length and continuity by serial reconstructions of 8 μm of the dorsal DD process (Figure 4A). MTs parallel to the axon were reconstructed as continuous tracks, while misoriented MTs were not continuous in adjacent sections and could not be reconstructed. Noticeably, *tba-1(gf) dlk-1(0)* showed a significant increase in the length of continuous MT tracks compared to wild type animals (Figure 4C, S4A).

To test how the increase in MT length and number observed in fixed EM samples affected MT dynamics in *tba-1(gf) dlk-1(0),* we imaged MT growth using fluorescently tagged EBP-2 (P_{unc-25}EBP-2::GFP). End Binding Proteins (EBPs) like EBP-2 transiently bind to the plus ends of growing (dynamic) MTs [15, 24], and EBP-2::GFP movement is recorded in movies and analyzed as tracks on kymographs (Movie S2, Figure 4E, F). We analyzed kymographs from both the proximal and distal DD neurites in the VNC of adult animals. As the *unc-25* promoter labels both DD and VD neurons, these kymographs also included information from the proximal VD neurites (Figure 4D). The EBP-2::GFP track velocity, run length, direction and number were equivalent in both proximal and distal neurites; so the data were pooled for further analysis. We observed a striking reduction in the number of EBP-2::GFP tracks in *tba-1(gf) dlk-1(0)* compared to wild type animals (Figure 4F, H), even as the steady state fluorescence intensity of EBP-2::GFP was indistinguishable between wild type and *tba-1(gf) dlk-1(0)* (Figure S4C, D). The reduction in dynamic MTs was not restricted to the VNC; the number of tracks in the commissures and DNC were also reduced in *tba-1(gf) dlk-1(0)* (Figure S4E-H and data not shown). The run length of EBP-2::GFP tracks was increased in *tba-1(gf) dlk-1(0)* (Figure 4I) while MT growth velocity was reduced (Figure 4J), indicative of more persistent MT growth than wild type. The reduction in EBP-2::GFP tracks, together with the increased number and length of MTs in fixed EM samples, indicates a loss in balance in the number of stable and dynamic MTs in *tba-1(gf) dlk-1(0).*

An increase in dynamic MTs facilitates DD remodeling

To address whether changes in MT dynamics correlated with DD remodeling, we imaged EBP-2::GFP in L1 animals before and after the onset of DD remodeling (6-8 hph and 12-14 hph, respectively; Figure 5A-E). The VD neurons were not born at both time points, allowing us to assay changes in MT dynamics only in the DD neurites. Before DD remodeling, wild type and *tba-1(gf) dlk-1(0)* animals had similar numbers of EBP-2::GFP tracks (Figure 5B-D). At the onset of DD remodeling, wild type animals showed a significant increase in the number of growing MTs (Figure 5B, D). In contrast, we observed

no significant difference in MT dynamics in *tba-1(gf) dlk-1(0)* before and after the onset of remodeling (Figure 5C, D). We also found that in the ventral DD processes of both larval (Figure 5E) and adult (Figure 4G) animals, >80% of the EBP-2::GFP tracks moved in the anterograde direction, indicating that MT polarity in DD neurons was unchanged during remodeling. These data suggest that changes in MT dynamics, but not polarity, are necessary for DD remodeling.

We then asked if altering MT dynamics could directly affect DD remodeling. Nocodazole is an MT destabilizing drug shown to be effective in *C. elegans* motor neurons [25]. We treated L1 animals with 10 μM nocodazole before DD remodeling, and then placed them on drug free plates until adulthood. The number of dynamic MTs was increased in adult animals following nocodazole treatment, while MT polarity was unchanged compared to control animals (Figure 5H-J). Adult DD neurons in nocodazole treated wild type animals also formed synapses along the DNC (Figure 5F, G). Importantly, in *tba-1(gf) dlk-1(0)*, such acute nocodazole treatment significantly rescued the failure in DD remodeling, with fewer synaptic puncta retained along the VNC and increased synaptic puncta along the DNC, compared to control animals (Figure 5F, G). Together, these findings support a conclusion that an increase in the number of dynamic MTs in DD neurons promotes synapse remodeling.

Gain-of-function kinesin-1 mutations suppress the DD remodeling defects of *tba-1(gf) dlk-1(0)*

To gain further insight into how MT dynamics regulate DD remodeling, we screened for EMS-induced mutations that suppressed the synaptic and behavioral defects of *tba-1(gf) dlk-1(0)*. We identified two mutations (*ju972* and *ju977*) (Figure 6A-C) that affect the gene *unc-116*, the heavy chain of the anterograde motor KIF5/kinesin-1. *ju972* alters a conserved Gly274 to Arg in the motor domain, and *ju977* alters a conserved Glu432 to Lys in the coiled-coil Rod 1 domain, which acts as a flexible hinge affecting motor motility [26] (Figure 6C, S5A).

We rescued the suppression of the behavioral and synaptic defects of *tba-1(gf) dlk-1(0)* by *ju972* and *ju977* by overexpressing wild type UNC-116 (Figure 6D, E). Conversely, overexpression of UNC-116(G274R) and UNC-116(E432K) in *tba-1(gf) dlk-1(0)* suppressed both behavioral and synaptic defects (Figure 6D, E). These results demonstrate that *unc-116(ju972)* and *unc-116(ju977)* caused the behavioral and synaptic suppression of *tba-1(gf) dlk-1(0)*. The reduction in synapse number seen in *tba-1(gf)* alone was not suppressed by either *unc-116(ju972)* or *unc-116(ju977)* (Figure 6A, B), and neither mutation showed any effect in *dlk-1(0)* (Figure 6A, B). Together, these genetic data show that the *unc-116* mutations specifically suppress the synergistic remodeling defects of *tba-1(gf) dlk-1(0).*

Previously characterized *unc-116* alleles range from being mildly uncoordinated to almost paralyzed, with severe defects in synapse development and organelle trafficking [27, 28]. In contrast, *unc-116(ju972)* and *unc-116(ju977)* showed wild type locomotion and normal GABAergic synapse development (Figure 6 A, B and data not shown). Both alleles also complemented other hypomorphic *unc-116* alleles in locomotion and synapse development

(data not shown). Moreover, analysis of immunostaining for endogenous UNC-116 revealed no discernable changes in protein localization in these two mutants (Figure S5B). These data indicate that both *ju972* and *ju977* are gain-of-function mutations of *unc-116* (designated as *unc-116(gf)*).

Several *unc-116* loss-of-function alleles, including *unc-116(e2310)*, decrease MT transport and alter MT polarity in *C. elegans* bipolar DA motor neurons [28]. However, we found that *unc-116(e2310)* did not suppress the behavioral or synaptic remodeling defects of *tba-1(gf) dlk-1(0)* animals (data not shown). Imaging of EBP-2::GFP in *unc-116(ju972)* revealed no effects on MT polarity in DD neurons (Figure S5C, D), or increase the number of dynamic MTs in *tba-1(gf) dlk-1(0)* (Figure S5C, E). Thus, these observations suggest that the *unc-116(gf)* mutations do not alter neuronal MTs in the DD neurons, and instead compensate for the DD remodeling defect in *tba-1(gf) dlk-1(0)* through a different mechanism.

To understand how the *unc-116(gf)* mutations might affect kinesin-1 function and suppress *tba-1(gf) dlk-1(0)*, we modeled the motor domain of UNC-116. We found that G274 (mutated to arginine in *unc-116(ju972)*) was a conserved residue in the MT binding domain (L12/α5) of the motor [29] (Figure 7A), and could potentially affect MT-motor affinity. A previous alanine scan of the MT binding domain of human kinesin-1 found that mutating residue Glu270 (Glu273 in UNC-116) to alanine resulted in increased affinity of the motor domain to MTs [29]. Since Glu273 is next to Gly274, we attempted to phenocopy the suppression of *tba-1(gf) dlk-1(0)* by *unc-116(gf)* using UNC-116(E273A). *tba-1(gf) dlk-1(0)* animals that expressed UNC-116(E273A) remodeled their DD synapses to a similar extent as animals that transgenically expressed UNC-116(G274R) or contained *unc-116(ju972)* (Figure 7B). As a control, overexpressing wild type UNC-116 did not rescue the DD remodeling defect of *tba-1(gf) dlk-1(0)*. These observations suggest that the suppressing activity of the *unc-116(gf)* alleles on *tba-1(gf) dlk-1(0)* could be due to increased MT-motor affinity that compensated for the MT defects in *tba-1(gf) dlk-1(0)* animals.

Synaptic vesicle transport during remodeling requires dynamic MTs

Anterograde motors of the kinesin superfamily drive axonal transport of various membrane organelles, including synaptic vesicle precursors [30]. The kinesin motors of the kinesin-3 subfamily (UNC-104 in *C. elegans*) are generally thought to be the major motors involved in axonal synaptic vesicle precursor transport. Indeed, reducing *unc-104* function completely blocks synaptic vesicle precursor transport in *C. elegans* [31]. However, multiple studies also show that kinesin-1 motors regulate synaptic vesicle precursor transport [24, 27]. To test the interaction of *unc-116(gf)* with *unc-104* in synaptic vesicle transport, we constructed *unc-104(lf); unc-116(ju972)* and *unc-104(lf); unc-116(ju977)* double mutant animals. We observed that the synaptic vesicle transport defects of *unc-104(lf)* animals were partially suppressed by both *unc-116(gf)* alleles, indicated by the increase in synaptic puncta along the VNC (Figure 7C, D), suggesting that *unc-116(gf)* could play a direct role in synaptic vesicle transport. We then hypothesized that the *unc-116(gf)* alleles might compensate for the block in synaptic vesicle precursor transport resulting from the loss of dynamic MTs in *tba-1(gf) dlk-1(0)*. To test this idea, we assayed synaptic vesicle transport in DD neuron

commissures during remodeling (14-18 hph). In wild type animals, we observed SNB-1::GFP labeled vesicles moving in anterograde (towards the DNC) and retrograde directions, with a strong anterograde bias (Movie S3, Figure 7F, G). The average velocity (~1.1 μm/s) and proportion of anterogradely moving vesicles was unchanged in *tba-1(gf) dlk-1(0)* and *tba-1(gf) dlk-1(0); unc-116(ju977)* animals, compared to wild type (Figure 7G). Interestingly, there was a significant reduction in the number of mobile vesicles in *tba-1(gf) dlk-1(0)*, which was reversed in *tba-1(gf) dlk-1(0); unc-116(ju977)* (Figure 7H), indicating that *tba-1(gf) dlk-1(0)* altered kinesin-1 movement to affect synaptic vesicle transport during remodeling. Since the loss of dynamic MTs was responsible for defective synapse remodeling in *tba-1(gf) dlk-1(0)*, we conclude that dynamic microtubules promote kinesin-1 dependent synaptic vesicle transport during synapse remodeling.

Discussion

Synapse remodeling is an essential process in the development of mature neuronal circuits in many animals, including humans [32]. However, whether cytoskeletal changes underlie the coordinated elimination and formation of synapses has not been well addressed. Synapse remodeling in *C. elegans* DD neurons is a precisely timed process, with synaptic connectivity changes achieved in the complete absence of neurite remodeling [7, 10]. Using this model, we have discovered that dynamic MTs are required for coordinating motor movement and synaptic vesicle transport during circuit rewiring.

By imaging MT growth, we show that while the ventral process of the DD neuron switches from an axonal to a dendritic identity during remodeling, MT polarity remains plus end out, a typically axonal polarity for many organisms [2]. Instead, our data reveal that changes in MT stability are critical for DD remodeling. An increase in dynamic MTs in wild type animals correlated with the onset of DD remodeling. In contrast, *tba-1(gf) dlk-1(0)* animals showed no change in the number of dynamic MTs in the same developmental time window, and were defective in DD remodeling. Ultrastructural analysis suggests that the loss of dynamic MTs in *tba-1(gf) dlk-1(0)* is likely due to increased MT stability. Supporting this idea, acute nocodazole treatment, which resulted in increased MT dynamics, could rescue defective DD remodeling in *tba-1(gf) dlk-1(0)*. Although MTs in mature axons are predominantly stable, it is being increasingly appreciated that dynamic MTs are important for a variety of neuronal processes, including axon regeneration [15, 33], dendritic spine growth [34] and memory formation [35]. Our studies reveal a specific role for dynamic MTs in modulating plasticity of pre-synaptic terminals, independent of axon outgrowth.

The DLK family of kinases regulates many aspects of nervous system development and response to injury [12-18]. The idea that DLK-1 is triggered by cytoskeletal instability has been documented in a variety of contexts [16, 18]. By genetically altering the MT cytoskeleton using *tba-1(gf)*, we find that *dlk-1* is necessary for DD remodeling. Transient activation of *dlk-1* at the onset of remodeling promotes the formation of new synapses during DD remodeling, which are maintained to adulthood. It is interesting to note that a few synaptic vesicles were transiently observed in the DNC of *tba-1(gf) dlk-1(0)* animals in the late larval stages. It is likely that the stabilization and maintenance of new synaptic sites is dependent on the transport of sufficient numbers of vesicles, consistent with similar findings

in cultured mammalian neurons [36, 37]. Moreover, induction of *dlk-1* expression in the late larval stages did not cause the stabilization of nascent dorsal synapses in *tba-1(gf) dlk-1(0)*, implying that *dlk-1* is not involved in the maintenance of new synapses. We propose that transient activation of DLK-1, through its target p38/PMK-3, regulates the activity of MT catastrophe factors like KLP-7 and SPAS-1 in the upregulation of dynamic MTs to promote new synapse formation.

Synaptic plasticity relies on regulated axonal transport of synaptic components along MTs, and a key player in this process is kinesin-1 [38, 39]. We identified novel kinesin-1 mutations that suppress the DD remodeling defects in *tba-1(gf) dlk-1(0)* animals, without altering their MT composition. Our data suggest that these gain-of-function kinesin-1 alleles increase the MT binding affinity, and in turn, the processivity of the motor to compensate for reduced synaptic vesicle transport in *tba-1(gf) dlk-1(0)*. Modifications in MT-motor affinity have important consequences in disease pathology, as mutations in the mammalian kinesin Kif21A that alter MT-motor binding have been found to cause oculo-motor axon stalling [40]. A recent study also reported that an increase in the overall negative charge of the C-terminal H12 helix of another *C. elegans* α-tubulin, MEC-12, increased the MT binding affinity of the minus end directed motor dynein, resulting in synaptic vesicle mistargeting in mechanosensory neurons [41]. This result differs from our findings in that an increase in the positive charge of the kinesin-1 motor suppresses synaptic vesicle trafficking defects of *tba-1(gf) dlk-1(0)* double mutants, even though *tba-1(gf)* increases the net positive charge of the H12 helix. However, we note that neither G274R nor E432K mutations, located on the motor head and coiled-coil Rod 1 domain of kinesin-1, respectively, show any effect on *tba-1(gf)* single mutants, and both suppress *tba-1(gf) dlk-1(0)* to the same extent. Hsu *et al* [41] also observed that simply increasing the overall positive charge of the H11-H12 loop, using a MEC-12(G416R) mutation, did not significantly change synaptic vesicle targeting in the mechanosensory neurons, consistent with our findings. We speculate that the loss of dynamic MTs in *tba-1(gf) dlk-1(0)* affects MT-motor interactions more profoundly than *tba-1(gf)* alone, and further investigation will be required to tease apart the various factors that affect MT-motor interactions in different cellular contexts *in vivo*.

Our observations also highlight the importance of MT dynamic instability in kinesin-1 mediated transport. MT-PTMs like tyrosination and acetylation have been associated with modulating kinesin-1 binding and velocity [23]. Although we did not detect gross changes in MT-PTMs in *tba-1(gf) dlk-1(0)*, we find that modulation of MT dynamics using nocodazole could rescue defective DD remodeling, indicating that any changes in MT-PTMs were secondary to an increase in the dynamic MT population. In cultured hippocampal neurons, kinesin-1 displays increased affinity to the axon initial segment, which is rich in dynamic MTs, to regulate polarized axonal transport [42]. A recent study also found preferential binding of kinesin-1 to GTPγS MTs, which are believed to mimic the plus ends of growing MTs [43, 44]. These observations, together with this study, support the idea that growing MTs themselves promote kinesin-1 dependent axonal transport. Up-regulation of kinesin-1 is essential for learning induced synaptic changes [39]. Our findings underscore the importance of dynamic MTs in coordinating motor and cargo interactions necessary for structural synaptic plasticity.

Experimental Procedures

C. elegans culture

Strains were maintained at 20°C on NGM plates unless noted otherwise. Information on alleles and genotypes of strains is summarized in Supplementary Experimental Procedures. To collect L1 animals, 20-30 gravid adults were placed on a seeded NGM plate to allow egg-laying for 2hrs. The hatched L1s were collected 10 hrs later. *tba-1(gf)* and *tba-1(gf)dlk-1(0)* animals showed a 10-12 hrs delay from egg lay to hatching, thus hatched L1s were collected 22 hrs later.

Fluorescent imaging of synapses and axons

L4 animals of the relevant genotypes were cultured at 20°C overnight, and day 1 adults were imaged using a Zeiss LSM 710 confocal microscope. Animals were anaesthetized in 0.6 mM levamisole on 2% agar pads for image acquisition. Z-stacks were generated from slices of 0.6 μm thickness. Images were processed using Zen lite software. Synaptic puncta and axon outgrowth defects were quantified manually using a Zeiss Axioplan 2 microscope equipped with Chroma HQ filters. For information on antibodies and EBP-2::GFP imaging, refer Supplementary Experimental Procedures.

SNB-1::GFP trafficking

L2 stage animals (14-18 hrs post hatching at 20°C) were collected for analysis, and anesthetized using 30 mM muscimol on 10% agarose pads. 4-D imaging was performed using a Yokogawa CSU-X1 spinning disc confocal head placed on a Nikon Eclipse Ti confocal microscope equipped with a piezo Z stage for fast Z-acquisition and a Hamamatsu Lineage EMx2-IK camera (1,024×1,024 active pixels), controlled using μManager. The entire DD commissure was visualized in 5-6 slices (180 ms/slice), and images were collected for 20 frames with an interval of 300 ms between each frame. The resulting movies were analyzed using Metamorph (Molecular Devices) to generate kymographs for analysis of number, velocity and direction of movement of synaptic vesicles. Particles with a velocity <0.5 μm/s were removed from the analysis.

Nocodazole treatment

L1 animals were placed on seeded 10 μM nocodazole, or buffer control (M9 containing DMSO) plates and incubated for 9 hrs at 20°C. The animals were then transferred to unseeded plates for 10 minutes to remove bacteria containing the drugs and subsequently moved to fresh seeded NGM plates until day 1 adult stage. These animals were then used for imaging synaptic remodeling and microtubule dynamics.

Statistical Analysis

Statistical analysis was performed using GraphPad Prism 5. Normal distribution of samples was tested using D'Agostino & Pearson omnibus normality test. Significance was determined using unpaired t-tests for two samples, One way ANOVA followed by Tukey's multiple comparison tests and two way ANOVA followed by Bonferroni posttests for multiple samples.

Supplementary Material

Refer to Web version on PubMed Central for supplementary material.

Acknowledgments

We are grateful to A. Desai, S. Roy, Y. Zou, S. Halpain and members of our labs for advice and helpful discussions. We thank A. D. Chisholm, W. Knowlton, K.W. Kim, M. Chuang, M. Andrusiak, K. Noma, S. Takayanagi-Kiya and Z. Wang for comments on the manuscript. We thank F. McNally for anti-UNC-116 antibodies, G. Peeters for use of a spinning disk confocal microscope, E. Jorgensen for *oxEx1268* line, the Caenorhabditis Genetics Center and the Mitani lab (Tokyo Women's Medical College) for strains. Y.J. is an Investigator, and A. G. and D. Y. were research associates, of the Howard Hughes Medical Institute. N. K. was a recipient of the Latham & Watkins Graduate Fellowship. This work was supported by HHMI and an NIH grant (NINDS R01 035546 to Y. J.).

References

1. Destexhe A, Marder E. Plasticity in single neuron and circuit computations. Nature. 2004; 431:789–795. [PubMed: 15483600]
2. Conde C, Cáceres A. Microtubule assembly, organization and dynamics in axons and dendrites. Nature reviews Neuroscience. 2009; 10:319–32.
3. Hummel T, Krukkert K, Roos J, Davis GW, Klambt C. *Drosophila* Futsch / 22C10 is a MAP1B-like protein required for dendritic and axonal development. Neuron. 2000; 26:357–370. [PubMed: 10839355]
4. Roos J, Hummel T, Ng N, Klambt C, Davis GW. *Drosophila* Futsch regulates synaptic microtubule organization and is necessary for synaptic Growth. Neuron. 2000; 26:371–382. [PubMed: 10839356]
5. Nahm M, Lee M-J, Parkinson W, Lee M, Kim H, Kim Y-J, Kim S, Cho YS, Min B-M, Bae YC, et al. Spartin regulates synaptic growth and neuronal survival by inhibiting BMP mediated microtubule stabilization. Neuron. 2013; 77:680–695. [PubMed: 23439121]
6. Harris KM, Weinberg RJ. Ultrastructure of Synapses in the Mammalian Brain Ultrastructure of Synapses in the. Cold Spring Harb Perspect Biol. 2012; 4:a005587. [PubMed: 22357909]
7. White JG, Albertson DG, Anness MAR. Connectivity changes in a class of motorneurons during the development of a nematode. Nature. 1978; 271:764–766. [PubMed: 625347]
8. White JG, Southgate E, Thomson JN, Brenner S. The Structure of the Nervous System of the Nematode *Caenorhabditis elegans*. Philosophical Transactions of the Royal Society B: Biological Sciences. 1986; 314:1–340.
9. Zhou HM, Walthall WW. UNC-55, an orphan nuclear hormone receptor, orchestrates synaptic specificity among two classes of motor neurons in *Caenorhabditis elegans*. J. Neurosci. 1998; 18:10438–44. [PubMed: 9852581]
10. Hallam SJ, Jin Y. *lin-14* regulates the timing of synaptic remodeling in *Caenorhabditis elegans*. Nature. 1998; 395:644–647.
11. Park M, Watanabe S, Poon VYN, Ou C-Y, Jorgensen EM, Shen K. CYY-1/cyclin Y and CDK-5 differentially regulate synapse elimination and formation for rewiring neural circuits. Neuron. 2011; 70:742–57. [PubMed: 21609829]
12. Nakata K, Abrams B, Grill B, Goncharov A, Huang X, Chisholm AD, Jin Y. Regulation of a DLK-1 and p38 MAP kinase pathway by the ubiquitin ligase RPM-1 is required for presynaptic development. Cell. 2005; 120:407–20. [PubMed: 15707898]
13. Yan D, Wu Z, Chisholm AD, Jin Y. The DLK-1 kinase promotes mRNA stability and local translation in C. elegans synapses and axon regeneration. Cell. 2009; 138:1005–18. [PubMed: 19737525]
14. Welsbie DS, Yang Z, Ge Y, Mitchell KL, Zhou X, Martin SE, Berlinicke CA, Hackler L Jr. Fuller J, Fu J, et al. Functional genomic screening identifies dual leucine zipper kinase as a key mediator of retinal ganglion cell death. PNAS. 2013; 110:4045–4050. [PubMed: 23431148]

15. Ghosh-Roy A, Goncharov A, Jin Y, Chisholm AD. Kinesin-13 and tubulin posttranslational modifications regulate microtubule growth in axon regeneration. Developmental cell. 2012; 23:716–28. [PubMed: 23000142]
16. Bounoutas A, Kratz J, Emtage L, Ma C, Nguyen KC, Chalfie M. Microtubule depolymerization in *Caenorhabditis elegans* touch receptor neurons reduces gene expression through a p38 MAPK pathway. PNAS. 2011; 108:3982–3987. [PubMed: 21368137]
17. Klinedinst S, Wang X, Xiong X, Haenfler JM, Collins CA. Independent pathways downstream of the Wnd/DLK MAPKKK regulate synaptic structure, axonal transport, and injury signaling. J. Neurosci. 2013; 33:12764–78. [PubMed: 23904612]
18. Valakh V, Walker LJ, Skeath JB, DiAntonio A. Loss of the spectraplakin short stop activates the DLK injury response pathway in *Drosophila*. J. Neurosci. 2013; 33:17863–73. [PubMed: 24198375]
19. Baran R, Castelblanco L, Tang G, Shapiro I, Goncharov A, Jin Y. Motor neuron synapse and axon defects in a *C. elegans* alpha-tubulin mutant. PloS one. 2010; 5:e9655. [PubMed: 20300184]
20. Roll-mecak A, Mcnally FJ. Microtubule-severing enzymes. Current Opinion in Cell Biology. 2010; 22:96–103. [PubMed: 19963362]
21. Moores CA, Francis F, Chelly J, Houdusse A, Milligan RA, Jolla L, Mentaux R, et al. Mechanism of microtubule stabilization by doublecortin. Molecular Cell. 2004; 14:833–839. [PubMed: 15200960]
22. Houtman SH, Rutteman M, Zeeuw CIDE. Echinoderm microtubule associated protein like protein 4, a member of the echinoderm microtubule associated protein family, stabilizes microtubules. Neuroscience. 2007; 144:1373–1382. [PubMed: 17196341]
23. Janke C, Bulinski JC. Post-translational regulation of the microtubule cytoskeleton: mechanisms and functions. Nature reviews. Molecular cell biology. 2011; 12:773–86.
24. Mimori-Kiyosue Y, Shiina N, Tsukita S. The dynamic behavior of the APC-binding protein EB1 on the distal ends of microtubules. Current biology. 2000; 10:865–8. [PubMed: 10899006]
25. Chalfie M, Thomson JN. Structural and functional diversity in the neuronal microtubules of *Caenorhabditis elegans*. The Journal of cell biology. 1982; 93:15–23. [PubMed: 7068753]
26. Grummt M, Henningsen U, Fuchs S, Schleicher M, Schliwa M. Importance of a flexible hinge near the motor domain in kinesin-driven motility. The EMBO Journal. 1998; 17:5536–5542. [PubMed: 9755154]
27. Byrd DT, Kawasaki M, Walcoff M, Hisamoto N, Matsumoto K, Jin Y. UNC-16, a JNK-signaling scaffold protein, regulates vesicle transport in *C. elegans*. Neuron. 2001; 32:787–800. [PubMed: 11738026]
28. Yan J, Chao DL, Toba S, Koyasako K, Yasunaga T, Hirotsune S, Shen K. Kinesin-1 regulates dendrite microtubule polarity in *Caenorhabditis elegans*. eLife. 2013; 2:e00133–e00133. [PubMed: 23482306]
29. Woehlke G, Ruby a K. Hart CL, Ly B, Hom-Booher N, Vale RD. Microtubule interaction site of the kinesin motor. Cell. 1997; 90:207–16. [PubMed: 9244295]
30. Hirokawa N, Noda Y, Tanaka Y, Niwa S. Kinesin superfamily motor proteins and intracellular transport. Nature reviews. Molecular cell biology. 2009; 10:682–696.
31. Hall DH, Hedgecock EM. Kinesin-Related Gene unc-104 is required for axonal transport of synaptic vesicles in *C. elegans*. Cell. 1996; 65:837–847. [PubMed: 1710172]
32. Hensch TK. Critical period regulation. Annual review of neuroscience. 2004; 27:549–79.
33. Cho Y, Cavalli V. HDAC5 is a novel injury-regulated tubulin deacetylase controlling axon regeneration. EMBO Journal. 2012; 31:3063–78. [PubMed: 22692128]
34. Jaworski J, Kapitein LC, Gouveia SM, Dortland BR, Wulf PS, Grigoriev I, Camera P, Spangler SA, Stefano PD, Demmers J, et al. Dynamic microtubules regulate dendritic spine morphology and synaptic plasticity. Neuron. 2009; 61:85–100. [PubMed: 19146815]
35. Uchida S, Martel G, Pavlowsky A, Takizawa S, Hevi C, Watanabe Y, Kandel ER, Alarcon JM, Shumyatsky GP. Learning-induced and stathmin-dependent changes in microtubule stability are critical for memory and disrupted in ageing. Nature Communications. 2014; 5:1–13.
36. Jin Y, Garner CC. Molecular mechanisms of presynaptic differentiation. Annu. Rev. Cell Dev. Biol. 2008; 24:237–62. [PubMed: 18588488]

37. McAllister AK. Dynamic aspects of CNS synapse formation. Annu. Rev. Neurosci. 2007; 30:425–50. [PubMed: 17417940]

38. Cai Q, Pan PY, Sheng ZH. Syntabulin-kinesin-1 family member 5B-mediated axonal transport contributes to activity-dependent presynaptic assembly. J. Neurosci. 2007; 27:7284–96. [PubMed: 17611281]

39. Puthanveettil SV, Monje FJ, Miniaci MC, Choi Y.-beom, Karl KA, Khandros E, Gawinowicz MA, Sheetz MP, Kandel ER. A new component in synaptic plasticity : upregulation of Kinesin in the neurons of the gill-withdrawal reflex. Cell. 2008; 135:960–973. [PubMed: 19041756]

40. Cheng L, Desai J, Miranda CJ, Duncan JS, Qiu W, Nugent AA, Kolpak AL, et al. Human CFEOM1 mutations attenuate KIF21A autoinhibition and cause oculomotor axon stalling. Neuron. 2014; 82:334–349. [PubMed: 24656932]

41. Hsu J-M, Chen C-H, Chen Y-C, Mcdonald KL, Gurling M, Lee A, Garriga G, et al. Genetic analysis of a novel Tubulin mutation that redirects synaptic vesicle targeting and causes neurite degeneration in *C. elegans*. PLoS genetics. 2014; 10:e1004715. [PubMed: 25392990]

42. Nakata T, Hirokawa N. Microtubules provide directional cues for polarized axonal transport through interaction with kinesin motor head. The Journal of cell biology. 2003; 162:1045–55. [PubMed: 12975348]

43. Maurer SP, Bieling P, Cope J, Hoenger A, Surrey T. GTPγS microtubules mimic the growing microtubule end structure recognized by end-binding proteins (EBs). PNAS. 2011; 108:3988–3993. [PubMed: 21368119]

44. Bechstedt S, Brouhard GJ. Doublecortin recognizes the 13-protofilament microtubule cooperatively and tracks microtubule ends. Developmental cell. 2012; 23:181–92. [PubMed: 22727374]

Highlights

- Synapse remodeling requires dynamic MTs
- The MAPKKK DLK-1 promotes synaptic remodeling
- Kinesin-1 compensates for reduced dynamic MTs to promote vesicle trafficking

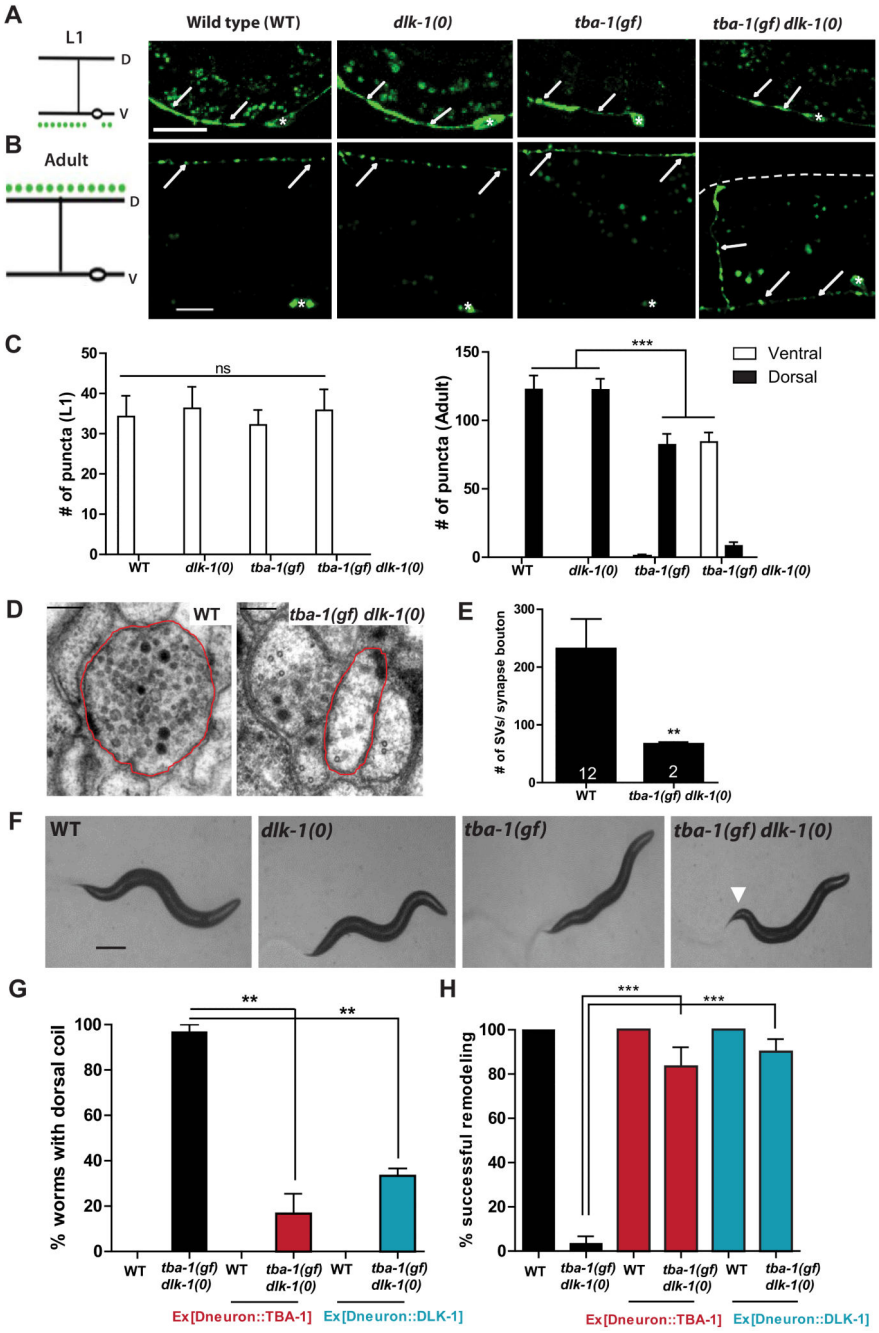

Figure 1. *tba-1(gf) dlk-1(0)* animals are defective in DD remodeling

(A, B) Representative images of DD synapses (P_{flp-13}-SNB-1::GFP (*juIs137*)) in L1 and adult animals. White arrows indicate the location of synaptic vesicles; white asterisks, DD cell bodies in the VNC; and dashed white line, the location of DNC in *tba-1(gf) dlk-1(0)*. Scale bars: 10 μm.

(C) Quantification of synaptic puncta in the VNC and DNC of L1 (left) and adult (right) animals. Data are mean ± SEM; n=10 animals per genotype. Statistics: One-Way ANOVA followed by Tukey's posttest; ***p<0.001, ns-not significant.

(D) Representative EM sections of DD neuron processes in the DNC. Axonal process of a DD neuron is outlined in red. Scale bar: 100 nm.
(E) Quantification of the number of synaptic vesicles in DD synapse boutons (sections containing an active zone). Data are mean ± SEM; n=number of synapse boutons (on graph). Statistics: unpaired t-test with Welch's correction; **p<0.01.
(F) Bright field images of the typical body posture on food. White arrow represents bent tail in *tba-1(gf) dlk-1(0)*. Scale bar: 200 μm.
(G, H) Cell autonomous rescue of the behavioral (G) and synapse remodeling (H) defects of *tba-1(gf) dlk-1(0)* using P_{unc-25} driven TBA-1 or DLK-1. Data are mean ± SEM; n=30 animals per genotype. Statistics: One-Way ANOVA followed by Tukey's posttest; **p<0.01, ***p<0.001. See also Figure S1.

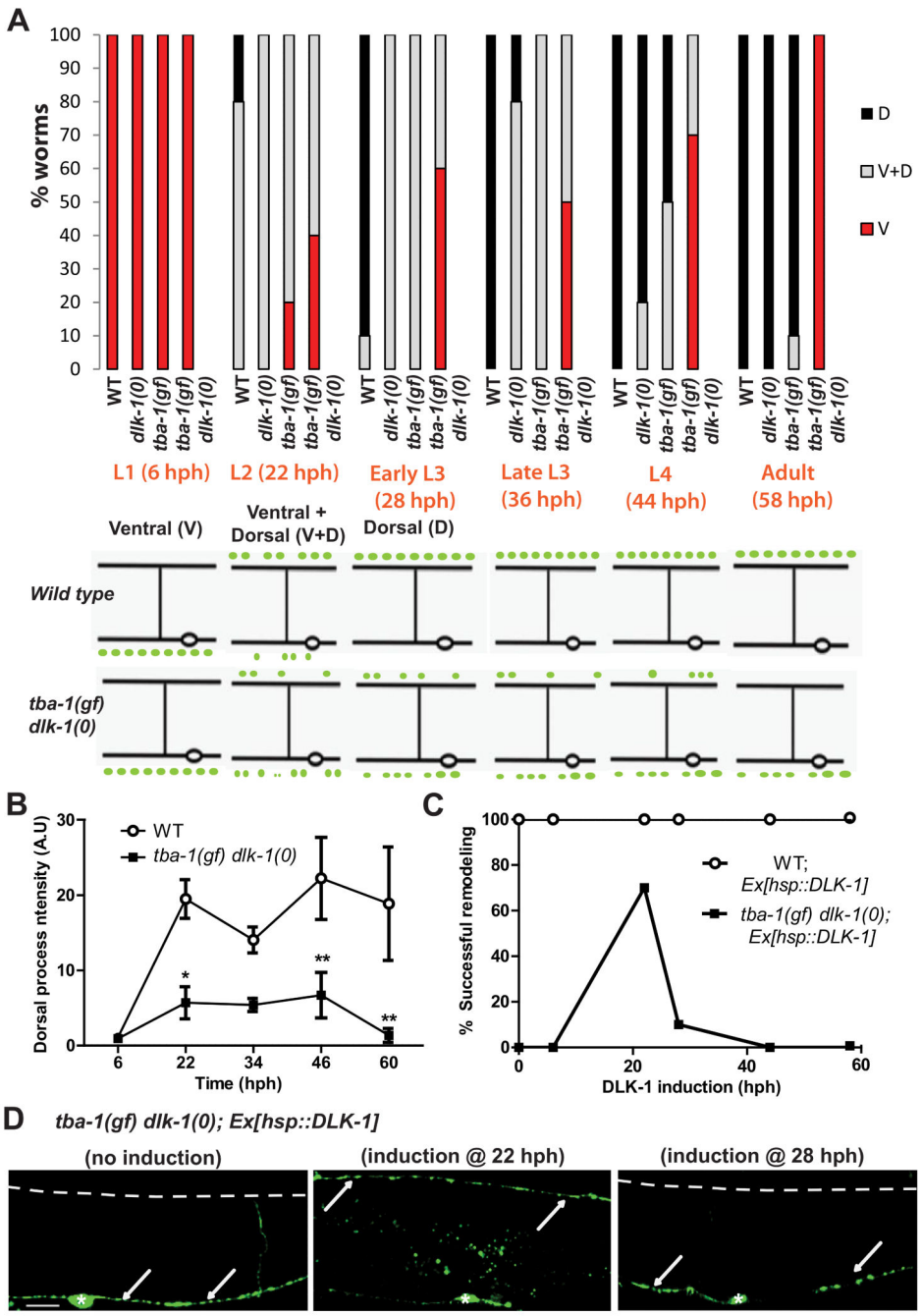

Figure 2. DLK-1 is required for establishing dorsal synapses during DD remodeling

(A) (Top) Progress of DD remodeling at 20°C from L1 (6 hph) to adult stages (56 hph) using *juIs137*. V: Synaptic puncta observed only along the VNC; V+D: synaptic puncta observed along both the VNC and DNC; D: synaptic puncta only along the DNC. n=10 animals per genotype for each time point. (Bottom) Schematic of DD remodeling. In WT, DD synapses are completely ventral (V) in the L1 stage, V+D in the L2 stage and then completely dorsal (D) after the L3 stage.

(B) *juIs137* intensity in the DNC during remodeling in WT and *tba-1(gf) dlk-1(0)* animals. Data are mean ± SEM; n=6 animals for each genotype per time point. Statistics: 2-way ANOVA followed by Bonferroni posttests; *p<0.05, **p<0.01.
(C) Rescue of DD remodeling defects in adult worms upon induction of DLK-1 at various larval stages in WT and *tba-1(gf) dlk-1(0)*; n=20 animals per genotype for each time point.
(D) Representative images of synapse location in an adult *tba-1(gf) dlk-1(0)* animal with no DLK-1 induction, DLK-1 induction at L2 stage (22 hph) and early L3 stage (28 hph). White arrows indicate the location of synaptic vesicles; dashed white line, the DNC; and white asterisks, DD cell bodies. Scale bar: 10 μm.

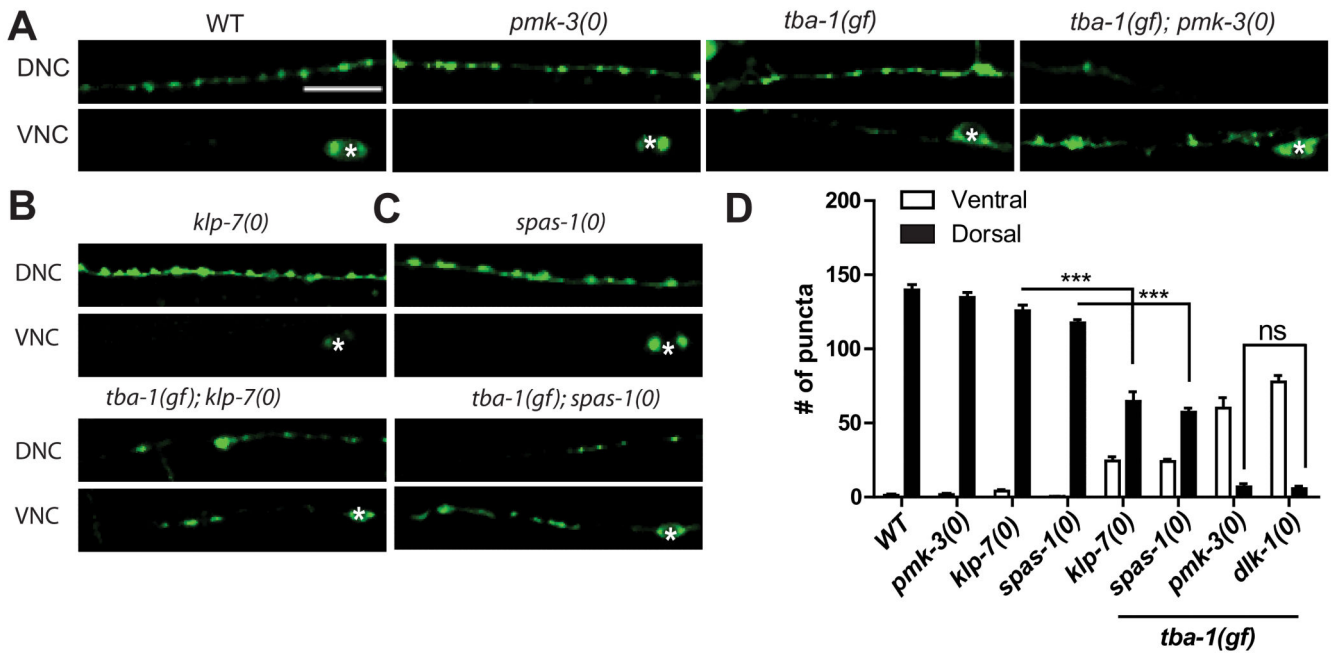

Figure 3. DLK-1 signals through PMK-3, and partly via KLP-7 and SPAS-1, in promoting DD remodeling

(A-C) Images of DD neuron synapses (*juIs137)* in genotype as indicated. White asterisk mark DD cell bodies on the VNC. Scale bars: 10 μm.

(D) Quantification of ventral and dorsal DD synaptic puncta. Data are represented as mean ± SEM; n=10 animals per genotype. Statistics: One-Way ANOVA followed Tukey's posttest; ***p<0.001, ns-not significant. See also Figure S2.

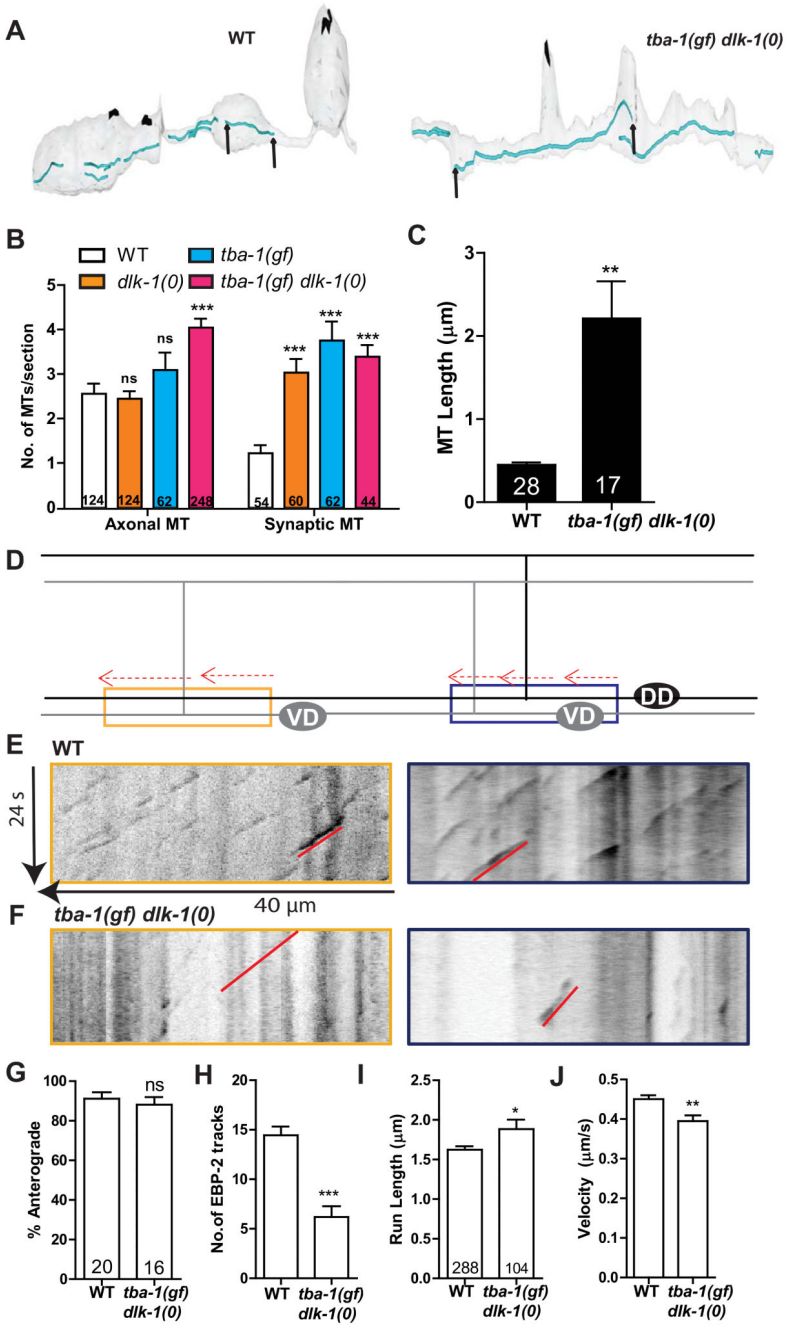

Figure 4. Dynamic MTs are reduced in *tba-1(gf) dlk-1(0)*

(A) Serial reconstruction of the dorsal processes of DD neurons in WT (~8 µm) and *tba-1(gf) dlk-1(0)* (~7.5 µm). Represented in blue are microtubules, and in black are active zones of pre-synaptic terminals. MT ends are indicated by black arrows.(B) MTs in DD neuron axonal (sections with no active zones) and synaptic (sections with active zones) sections. Data are mean ± SEM; n=# of sections for each genotype (graph). Statistics- 2-Way ANOVA followed by Bonferroni posttest; ***p<0.001, ns-not significant.

(C) MT length in the DNC of WT and *tba-1(gf) dlk-1(0)* DD neurons. Data are mean ± SEM; n=# of MTs (graph). Statistics - unpaired t-test with Welch's correction; **p<0.01.
(D) Schematic representation of EBP-2::GFP tracks (red) in the VNC of adult DD (black) and VD (gray) neurons, with proximal (blue) and distal (yellow) neurites used for imaging.
(E, F) Representative kymographs of MT dynamics from proximal (blue outline) and distal (yellow) DD neurites in (E) WT and (F) *tba-1(gf) dlk-1(0)* adults. Red line indicates a single EBP-2::GFP track moving in the anterograde direction.
(G-J) Quantification of (G) direction of movement, (H) number, (I) run length and (J) velocity of EBP-2::GFP tracks in the proximal and distal neurites. Data are mean ± SEM; n=# of animals in (G-H) and # of EBP-2::GFP tracks in (I-J). Statistics - unpaired t-test (with Welch's correction for (I)); ns-not significant, ***p<0.001, *p<0.05, **p<0.01. See also Figure S3 and S4.

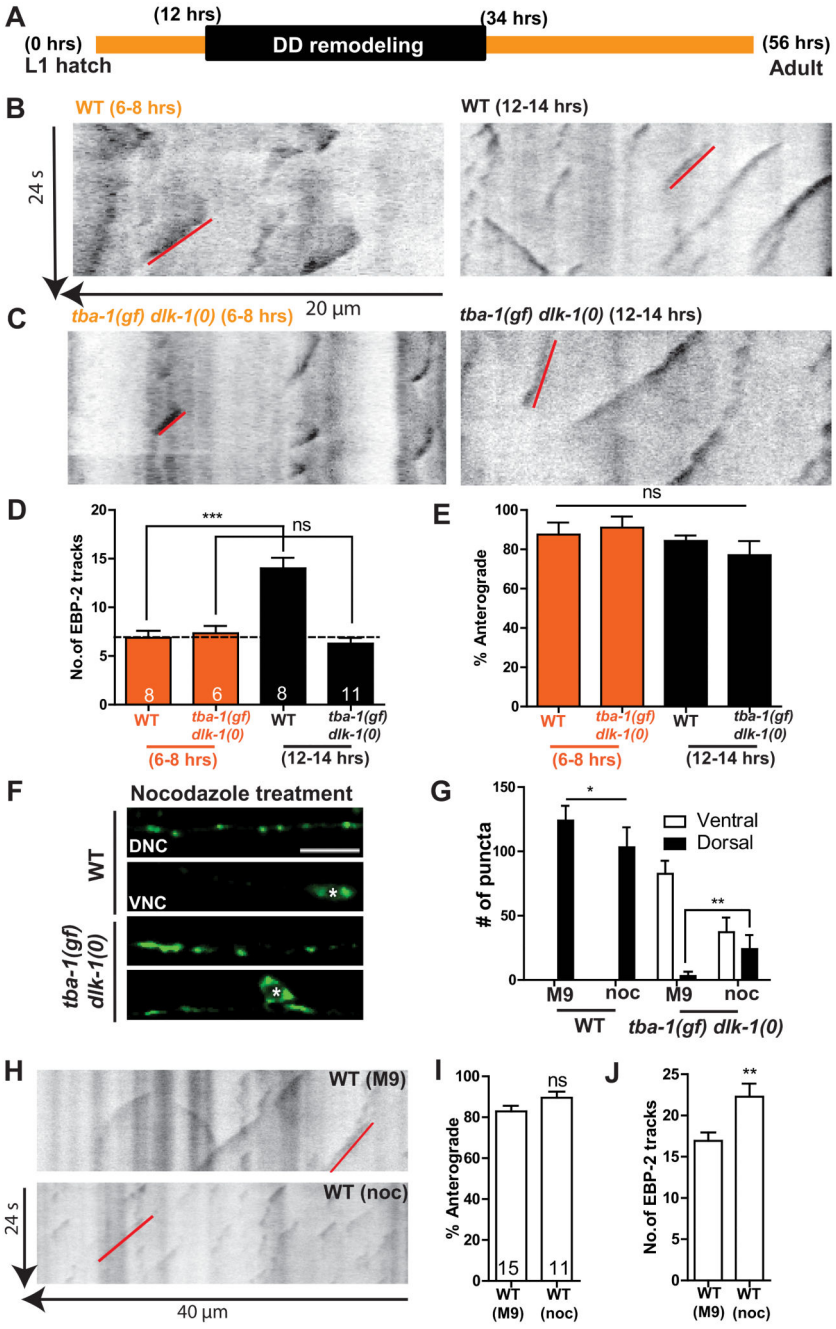

Figure 5. DD remodeling requires dynamic MTs

(A) Timeline of DD remodeling at 20°C.

(B, C) Representative kymographs of MT dynamics in WT and *tba-1(gf) dlk-1(0)* before (6-8 hph) and after (12-14 hph) the onset of DD remodeling. Red line represents a single EBP-2::GFP track moving in the anterograde direction.

(D, E) Quantification of the (D) number and (E) direction of movement of EBP-2::GFP tracks in WT and *tba-1(gf) dlk-1(0)* animals before and during DD remodeling. Data are

mean ± SEM; n=# of animals, shown in (D). Statistics – One way ANOVA followed by Tukey's posttest; ***p<0.001, ns-not significant.

(F) DD synapses (*juIs137)* in the VNC and DNC of WT and *tba-1(gf) dlk-1(0)* adults after acute 10 μM nocodazole treatment before DD remodeling. White asterisks represent DD cell bodies. Scale bar: 10 μm.

(G) Quantification of dorsal and ventral DD synaptic puncta distribution after acute M9 (buffer control) and nocodazole treatment. Data are mean ± SEM; n=10 animals per genotype for each drug treatment. Statistics – One way ANOVA followed by Tukey's posttest; *p<0.05, **p<0.01.

(H) Representative kymographs of EBP-2::GFP movement in the adult VNC of WT (buffer control) and WT (nocodazole treated) animals. Red line represents a single EBP-2::GFP track moving in the anterograde direction.

(I, J) Quantification of (I) direction of movement and (J) number of EBP-2::GFP tracks. Data are mean ± SEM; n=# of animals, shown on (I). Statistics - unpaired t-test; **p<0.01; ns-not significant.

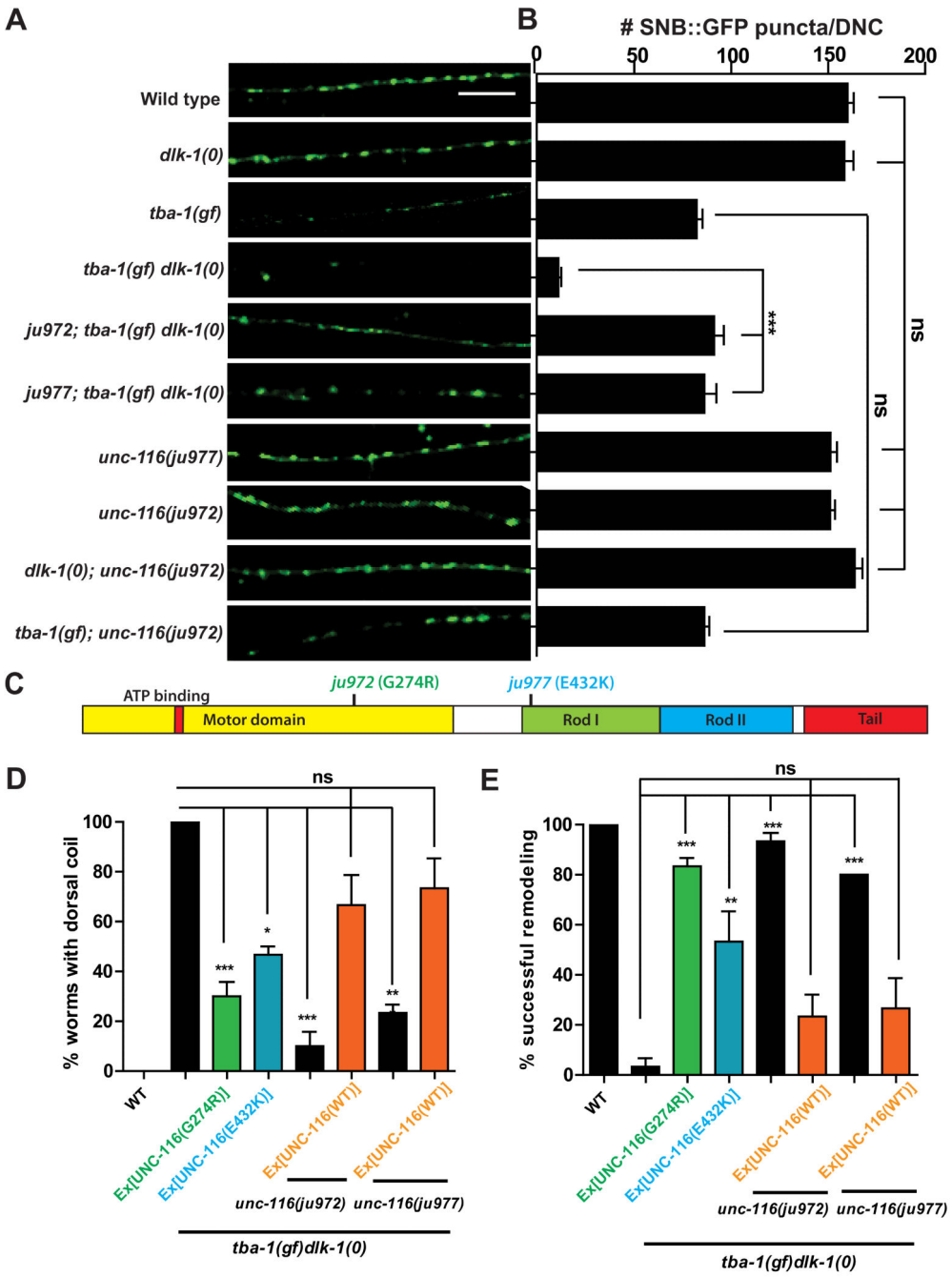

Figure 6. Gain-of-function kinesin-1 mutations suppress *tba-1(gf) dlk-1(0)*

(A) DD synapses in the adult DNC using P_{unc-25}-SNB-1::GFP (*juIs1*). Scale bar: 10 μm.

(B) Quantification of DD synapses in the DNC. Data are mean ± SEM; n=10 animals per genotype. Statistics - One-way ANOVA followed by Tukey's posttest; ***p<0.001, ns-not significant.

(C) UNC-116 protein domains; G274R (green) - *ju972*, E432K (blue) - *ju977*.

(D, E) Rescue of (D) behavioral and (E) synaptic defects of *tba-1(gf) dlk-1(0)* by transgenes expressing *ju972* or *ju977*. Data are mean ± SEM; n=30 animals per genotype. Statistics-

One way ANOVA followed by Tukey's posttest; ***p<0.001, ns-not significant. See also Figure S5.

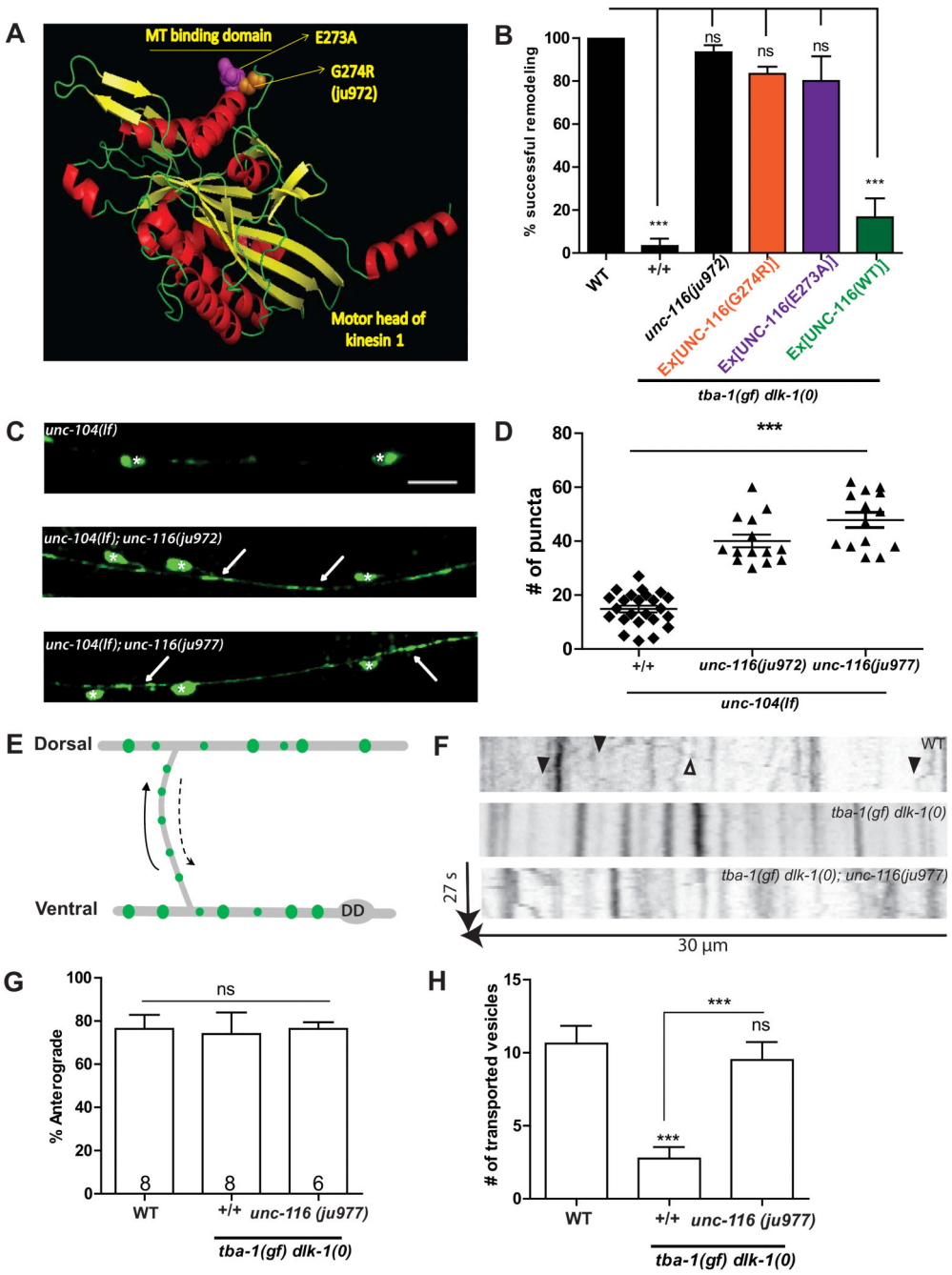

Figure 7. *unc-116(gf)* increases MT binding affinity to promote synaptic vesicle transport

(A) Prediction of the motor head of *C. elegans* UNC-116 (8-358aa) modeled on SWISS-MODEL and rendered using PyMOL.

(B) Rescue of DD remodeling defects of *tba-1(gf) dlk-1(0)* animals by transgenes expressing UNC-116(E273A). No rescue was observed with wild type kinesin-1 transgenes. Data are represented as mean ± SEM; n=30 animals per genotype. Statistics-One way ANOVA followed by Tukey's posttest; ***p<0.001; ns-not significant.

(C-D) Images and quantification of D neuron synapses in the VNC of *unc-104(lf), unc-104(lf); unc-116(ju972)* and *unc-104(lf); unc-116(ju977)* animals expressing *juIs1* (P_{unc-25}-SNB-1::GFP). White asterisks represent DD and VD cell bodies, white arrows indicate synapses. Scale bar: 10 μm. Statistics - unpaired t-test; ***p<0.001.
(E) Schematic of bidirectional synaptic vesicle transport along the commissure during DD remodeling. Solid arrow represents the anterograde direction, *i.e*, towards the DNC.
(F) Representative kymographs of synaptic vesicle transport along the DD commissure. Solid arrowheads indicate vesicles moving in the anterograde direction, and open arrowheads indicate vesicles moving in the retrograde direction.
(G, H) Quantification of (G) direction of movement and (H) number of mobile vesicles during DD remodeling. Data are mean ± SEM; n= no. of animals (shown on (G)). Statistics: One-way ANOVA followed by Tukey's posttest; ***p<0.001, **p<0.01, n.s.-not significant